



Contents lists available at ScienceDirect

## Journal of the Taiwan Institute of Chemical Engineers

journal homepage: [www.elsevier.com/locate/jtice](http://www.elsevier.com/locate/jtice)

Short communication

## Mixed convection flow of thermally stratified MHD nanofluid over an exponentially stretching surface with viscous dissipation effect

Prabhakar Besthapu<sup>a</sup>, Rizwan Ul Haq<sup>b,\*</sup>, Shankar Bandari<sup>a</sup>, Qasem M. Al-Mdallal<sup>c</sup><sup>a</sup> Department of Mathematics, Osmania University, Hyderabad, India<sup>b</sup> Department of Electrical Engineering, Bahria University, Islamabad Campus, Islamabad, Pakistan<sup>c</sup> Department of Mathematical Sciences, UAE University, P.O. Box 15551, Al Ain, United Arab Emirates

## ARTICLE INFO

## Article history:

Received 25 February 2016

Revised 6 December 2016

Accepted 20 December 2016

Available online xxx

## Keywords:

Stratification

Nanofluid

Dissipation

Permeable

Keller box

## ABSTRACT

The present analysis concentrates to examine the influence of both thermal and solutal stratification on magneto-hydrodynamics (MHD) nanofluid flow along an exponentially stretching sheet. Moreover, simultaneous effects of mixed convection and viscous dissipation are also analyzed to determine the thermal conductivity within the restricted domain. Energy and concentration equation consist of two important slip mechanisms, namely: the Brownian motion of nanoparticles and the thermophoresis due to concentration difference. By the mean of compatible similarity transformed, a system of PDEs is converted into the system of nonlinear ODEs. The resulting nonlinear ODEs are successfully solved via the implicit finite difference method (FDM). Obtained numerical solutions are plotted for each profile for different and converging values of including parameters. To validate the results, numerical values of Nusselt number are compared with the existing literature for a particular case. Obtained results present the significant impact of each parameter on temperature and concentration. Nanofluid flow behaviour is also observed via velocity profile.

© 2016 Taiwan Institute of Chemical Engineers. Published by Elsevier B.V. All rights reserved.

## 1. Introduction

Fluid flow past along a rough or flat surfaces attain a considerable attention by virtue of its extensive and considerable applications in engineering and manufacturing processes. Few important and foremost useful examples related to applications include the polymer extrusion, wires and fibre undercoat, food stuff wrapping, manufacturing of bags and papers, and petroleum manufacturing goods. Initially, Sakiadis [1] described the idea of boundary layer theory along a uniform moving surface that deals the free stream velocity and ambient fluid temperature is considered to be zero. Later on, Crane [2] has been examining the work for linear stretching velocity and it is proportional to the distance from the fixed slit. Thereafter the revolutionary idea presented by Crane has been extended by several other researchers by considering the various effects of heat and mass flow [3–5]. In the current decay, the most significant part of literature of fluid models is dealing with the linear stretching surface with various physical phenomena. However, Gupta and Gupta [3] established that all the physical phenomena need not to be dealt with linear but it can be dealt with the

exponential or non-linear stretching for both heat and mass transfer. They have further discovered that sheet can be considered as a permeable to deal the phenomena of suction and injection of the fluid.

Apart from all the fundamental problem of linear stretching sheet, existing literature also witnesses that flow examination due to exponentially stretching sheet is also an important factor in most of the manufacturing process. In the beginning, the idea of flow past over an exponentially stretching sheet is presented by Magyari and Keller [6]. They have found the numerical solution of fluid flow over a sheet that is stretched with exponential velocity that deals the phenomena of heat and mass transfer characteristics. In another study, Elbashareshy [7] extend the idea of Magyari and Keller [6] for exponential stretching sheet to deal the heat transfer with suction/injection effect. Currently many researchers have considered different and important ideas to deal the flow over an exponentially stretching surface for both Newtonian and non-Newtonian fluid models [8–15].

In the recent decay, heat transfer is one of the essential key features in the energy development at the industrial level and manufacturing process of any equipment. Despite of that fact heat addition, removing or transfer from one place to another place during the manufacturing process is totally based upon the thermal performance of working fluid. In several cases: water, engine oil,

\* Corresponding author.

E-mail addresses: [r.haq.qau@gmail.com](mailto:r.haq.qau@gmail.com), [ideal\\_riz@hotmail.com](mailto:ideal_riz@hotmail.com) (R.U. Haq), [q.almdallal@uaeu.ac.ae](mailto:q.almdallal@uaeu.ac.ae) (Q.M. Al-Mdallal).<http://dx.doi.org/10.1016/j.jtice.2016.12.034>

1876-1070/© 2016 Taiwan Institute of Chemical Engineers. Published by Elsevier B.V. All rights reserved.

### Nomenclature

$u, v$	velocity components in $x$ and $y$ directions (m/s)
$B$	magnetic induction (A/m) tesla
$U$	stretching velocity (m/s)
$U_0$	reference velocity (m/s)
$k$	thermal conductivity (W/m k)
$V_0$	strength of suction (m/s)
$T$	temperature of the fluid (K)
$T_w$	wall temperature (K)
$T_\infty$	ambient fluid temperature (K)
$C$	nanoparticle concentration (mol/m <sup>3</sup> )
$C_w$	nanoparticle concentration at the stretching surface (mol/m <sup>3</sup> )
$C_\infty$	nanoparticle ambient concentration (mol/m <sup>3</sup> )
$M$	Hartmann number
$Pr$	Prandtl number
$Le$	Lewis number
$Nt$	thermophoresis parameter
$Nb$	Brownian motion parameter
$Ec$	Eckert number
$S$	suction/injection parameter
$D_B$	Brownian diffusion coefficient (m <sup>2</sup> /s)
$D_T$	thermophoresis diffusion coefficient (m <sup>2</sup> /s)
$a, b, c, d$	are dimensional constants

### Greek symbols

$\eta$	similarity variable
$\alpha$	thermal diffusivity (m <sup>2</sup> /s)
$\nu$	kinematic viscosity of nanofluid (m <sup>2</sup> /s)
$\sigma$	electrical conductivity of nanofluid (S/m)
$\mu$	dynamic viscosity of nanofluid (kg / m s)
$\rho_f$	density of the fluid (kg/m <sup>3</sup> )
$(\rho c)_f$	capacity heat of the fluid (kg / m <sup>3</sup> K)
$(\rho c)_p$	capacity heat of the nanoparticles (kg / m <sup>3</sup> K)
$\varepsilon_1$	thermal stratification parameter
$\varepsilon_2$	solulal stratification parameter

researchers [36–38] for the flow due to a heated surface occupied due to stratified fluid. Thermal stratification produce when a uniform release of thermal boundary layer into the medium. Similarity solution attained by Kulkarni et al. [39], describe the natural convection flow near a heated plate for thermally stratified liquid. Plenty of the authors worked on the stratification with various effects [40–44].

The core part of this work is to analyse the influence of thermal and solulal stratification on nanofluid that moves over an exponential stretching sheet. For this, we have extended the idea of Khan and Pop [24] and modify it for double stratification phenomena in the form of PDEs. Transformed ODEs are solved via Keller box scheme. Effects of main emerging parameters are discussed graphically that based upon physical influence at velocity, temperature profile and concentration profiles. To highlight the results at the surface, results are also obtained for skin friction, Nusselt number and Sherwood number.

## 2. Mathematical model and formulation

It is considered that nanofluid flow is steady, incompressible, viscous, and two dimensional that past over a stretching sheet placed along  $x$ -axis while fluid is restricted in the domain  $y > 0$ . It is further assume that sheet is stretched with the exponential velocity  $U = U_0 e^{x/l}$ . We are further considering that sheet is permeable. Buoyancy forces are also considered for thermal and concentration to deal the double stratified phenomena. Since the surface is heated with the temperature  $T_w(x)$  and is embedded in a thermally stratified medium, and assume that the variable temperature  $T_w = T_0 + a e^{x/2l}$  and concentration  $C_w = C_0 + b e^{x/2l}$  at the surface and away from the sheet. Fig. 1 depicts the physical explanation of the given model. A variable magnetic field  $B(x) = B_0 e^{x/2l}$  is applied that is normal to the surface,  $B_0$  being constant. The governing equations for the above flow are

$$\frac{\partial u}{\partial x} + \frac{\partial v}{\partial y} = 0, \quad (1)$$

lubricants and other common working fluid have poor thermal conductivity as compare to the required conductivity at the industrial level. Incorporation of tiny particles within the working fluid plays an important to boost the poor thermal conductivity of base fluid. Choi [16] introduced a new class to raise the low thermal conductivity of any base fluid by dispersing tiny particles in the working fluids. Recently nanofluids have gained interest of researchers due its enhanced thermal conductivity property [17]. Buongiorno [18] identified seven slip mechanisms in which Brownian motion and thermophoresis are important factors. Some review studies concerning the analysis of nanofluids can be observed in [19–22]. Recently, Kuznetsov and Nield [23] extended the concept of Buongiorno [18] for boundary layer phenomena with the vertical wall. Later on, Khan and Pop [24] modify the concept of Brownian motion and thermophoresis for horizontal stretching surface. Currently, an extensive literature can be found for both Newtonian and non-Newtonian fluid with various physical models in the presence of nanoparticles [25–35].

Thermal and concentration stratification is one of the important and natural phenomena that occur due to the density difference. Most of the case, where the density of a material varies due to temperature difference or homogenous mixture changes its stats by providing the temperature then molecules having substantial density may accumulate at the base of the surface and molecules with low density switch and rise up at upper part of the layer. An experimental and analytical study has been done by several

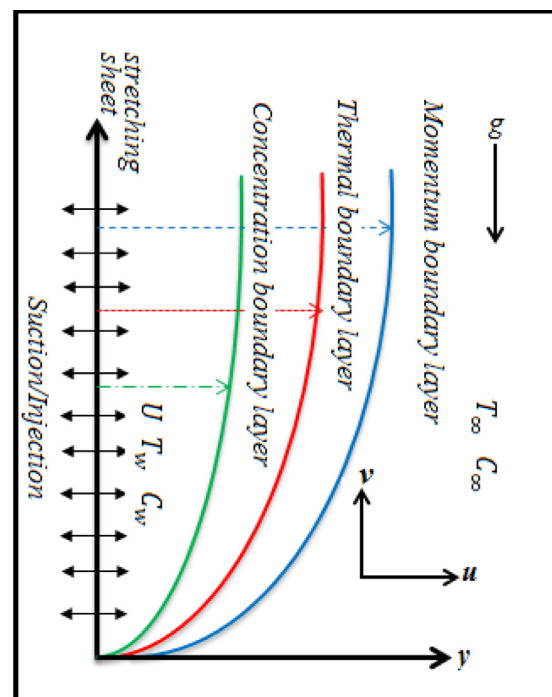


Fig. 1. Geometry of the model.

$$u \frac{\partial u}{\partial x} + v \frac{\partial v}{\partial y} = \nu_{nf} \frac{\partial^2 u}{\partial y^2} - \frac{\sigma B^2}{\rho_{nf}} u + \frac{g}{\rho_{nf}} \left\{ \rho_{f\infty} \beta_t (1 - C_\infty) (T - T_\infty) \right\} + \beta_c (\rho_p - \rho_{f\infty}) (C - C_\infty), \quad (2)$$

$$u \frac{\partial T}{\partial x} + v \frac{\partial T}{\partial y} = \alpha \frac{\partial^2 T}{\partial y^2} + \frac{(\rho c)_p}{(\rho c)_f} \left[ D_B \frac{\partial C}{\partial y} \frac{\partial T}{\partial y} + \frac{D_T}{T_\infty} \left( \frac{\partial T}{\partial y} \right)^2 \right] + \frac{v}{C_p} \left( \frac{\partial u}{\partial y} \right)^2, \quad (3)$$

$$u \frac{\partial C}{\partial x} + v \frac{\partial C}{\partial y} = D_B \frac{\partial^2 C}{\partial y^2} + \frac{D_T}{T_\infty} \frac{\partial^2 T}{\partial y^2}. \quad (4)$$

In above system of equation, involved expressions are defined in the nomenclature. The last term on the right hand side of energy Eq. (3) signifies the viscous dissipation. The appropriate boundary conditions for the flow problem are

$$u = U, \quad v = -V, \quad T = T_w(x), \quad C = C_w(x) \quad \text{at } y = 0, \quad (5)$$

$$u \rightarrow 0, \quad T = T_\infty(x) = T_0 + ce^{x/2l}, \quad C = C_\infty(x) = C_0 + de^{x/2l} \quad \text{as } y \rightarrow \infty. \quad (6)$$

Where  $U = U_0 e^{x/l}$  is the stretching velocity and  $U_0$  is the reference velocity,  $V(x)$  is the suction and injection velocity with  $V(x) = V_0 e^{x/2l}$  a special type of velocity at the wall is considered and  $V_0$  is the initial asset of the suction/injection.

By introducing the following similarity transformations

$$u = U_0 e^{x/l} f'(\eta), \quad v = -\sqrt{\frac{U_0}{2l}} e^{x/2l} \{f(\eta) + \eta f'(\eta)\}, \quad \eta = y \sqrt{\frac{U_0}{2vl}} e^{x/2l} \quad (7)$$

$$\theta(\eta) = \frac{T - T_\infty}{T_w - T_0}, \quad \phi(\eta) = \frac{C - C_\infty}{C_w - C_0} \quad (8)$$

Making use of the above transformations defined in Eqs. (7) and (8), it is found that Eq. (1) is identically satisfied and Eqs. (2)–(4) take the following form:

$$f''' + f f'' - 2f'^2 - 2M f' + 2\lambda_t (\theta + R\phi) = 0, \quad (9)$$

$$\theta'' + \text{Pr}(f\theta' - f'\theta - \varepsilon_1 f') + \text{Pr}Nb\theta'\phi' + \text{Pr}Nt\theta'^2 + \text{Pr}Ec f'^2 = 0, \quad (10)$$

$$\phi'' + \text{LePr}(f\phi' - f'\phi - \varepsilon_2 f') + \frac{Nt}{Nb}\theta'' = 0, \quad (11)$$

The adjacent boundary conditions defined in Eqs. (5) and (6) takes the following form,

$$f(0) = S, \quad f'(0) = 1, \quad \theta(0) = 1 - \varepsilon_1, \quad \phi(0) = 1 - \varepsilon_2, \quad f'(\infty) = 0, \quad \theta(\infty) = 0, \quad \phi(\infty) = 0. \quad (12)$$

It can be seen that if  $\varepsilon_1 = \varepsilon_2 = 0$  the present phenomena deals the unstratified case. Where, prime indicates the derivative with respect to similarity variable  $\eta$ . In the above system of equations:

$$M = \sqrt{2\sigma B_0^2 l / U_0 \rho}, \quad S = \frac{V_0}{\sqrt{\frac{U_0}{2vl}}}, \quad \text{Pr} = \frac{\nu}{\alpha}, \quad \text{Le} = \frac{\nu}{D_B},$$

$$Nt = \frac{D_T(T_w - T_0)(\rho c)_p}{T_\infty \nu (\rho c)_f}, \quad Nb = \frac{D_B(C_w - C_0)(\rho c)_p}{\nu (\rho c)_f}, \quad Ec = \frac{U^2}{C_p(T_w - T_0)},$$

$$\varepsilon_1 = \frac{c}{a}, \quad \varepsilon_2 = \frac{d}{b}, \quad \lambda_t = \frac{Gr_t}{Re_x^2}, \quad R = \frac{\lambda_c}{\lambda_T}, \quad \lambda_c = \frac{Gr_c}{Re_x^2},$$

$$Gr_t = \frac{g\rho f_\infty \beta_t (1 - C_\infty)(T_w - T_0)l x^2}{\rho_{nf} \nu^2},$$

**Table 1**

Comparison of  $-\theta'(0)$  for various values of Pr and M when Nb, Nt,  $\varepsilon_1$ ,  $\varepsilon_2$ , Ec all are zero.

M	Pr	Magyari and Keller [6]	Bidin and Nazar [11]	Ishak [14]	Present study
0	1	0.954782	0.9548	0.9548	0.9548
0	2		1.4714		1.4715
0	3	1.869075	1.8691	1.8691	1.8691
0	5	2.500135		2.5001	2.5001
0	10	3.660379		3.6604	3.6605
1	1			0.8611	0.8615

$$Gr_c = \frac{g\rho f_\infty \beta_c (\rho_p - \rho_{f\infty})(C_w - C_0)l x^2}{\rho_{nf} \nu^2}.$$

The physical quantities of interest are Nusselt and Sherwood numbers which are defined as:

$$Nu_x = -\frac{x}{(T_w - T_0)} \left( \frac{\partial T}{\partial y} \right)_{y=0}, \quad Sh_x = -\frac{x}{(C_w - C_0)} \left( \frac{\partial C}{\partial y} \right)_{y=0}$$

$$\sqrt{\frac{2L}{x}} Nu_x Re_x^{-1/2} = -\theta'(0), \quad \sqrt{\frac{2L}{x}} Sh_x Re_x^{-1/2} = -\phi'(0).$$

$$\text{Where } Re_x = \frac{xU_0 e^{x/l}}{\nu}.$$

### 3. Results and discussion

To solve the coupled nonlinear ordinary differential Eqs. (9)–(11) with associated boundary condition (12) is tackled numerically via finite difference method. This numerical scheme is discussed in detail by Cebeci and Bradshaw [45]. To determine the unknown profiles namely:  $f(\eta)$ ,  $\theta(\eta)$  and  $\phi(\eta)$  involving in the Eqs. (9)–(11) are determined via numerical technique that is mentioned above. These unknown profiles are plotted against the flow control parameters involved in the system of equations: namely magnetic parameter  $M$ , thermal stratified parameter  $\varepsilon_1$ , solutal stratified parameter  $\varepsilon_2$ , Brownian motion  $Nb$ , Prandtl number  $Pr$ , thermophoresis  $Nt$ , Lewis number  $Le$ , Eckert number  $Ec$ . The validation of the present method has been presented in Table 1 by comparing the values of Nusselt number in terms of  $-\theta'(0)$  for various values of Pr in the absence of nanoparticles and in an un-stratified environment i.e.  $\varepsilon_1 = 0 = \varepsilon_2$ .

In order to analyse the results, numerical computation is performed and obtained the results which are described graphically in Figs. 2–14. Fig. 2 depicts the velocity, temperature and nanoparticle concentration profile against the similarity variable  $\eta$  for distinct values of Hartmann number  $M$ . It has been described in many physical phenomena that magnetic field reduces the velocity of fluid particles. Physically, we can say that a resistive force that applies normal to surface of the sheet and hence reduces the motion of fluid. It is also depicts that rise in magnetic force leads to enhance the temperature and concentration distribution. Due to stronger Lorentz force, both temperature and concentration profile attaining the increasing behaviour with the increment in Hartmann number  $M$ . Influence of suction/injection parameter  $S$  on  $f(\eta)$ ,  $\theta(\eta)$  and  $\phi(\eta)$  are presented in Fig. 3. It is observed that both suction and injection case, results obtained for each velocity, temperature and concentration profile shows the increasing behaviour. It can further observed that results presented in Fig. 3 describe the significant distribution in concentration profile based upon high concentration is obtained when the fluid is blowing or injecting. It is obtained that in the vicinity of the surface, concentration profile rise significantly and later it is vanishing for higher values of similarity variable  $\eta$ . On the other hand it can be founded in the inset-II that results obtained for temperature and velocity

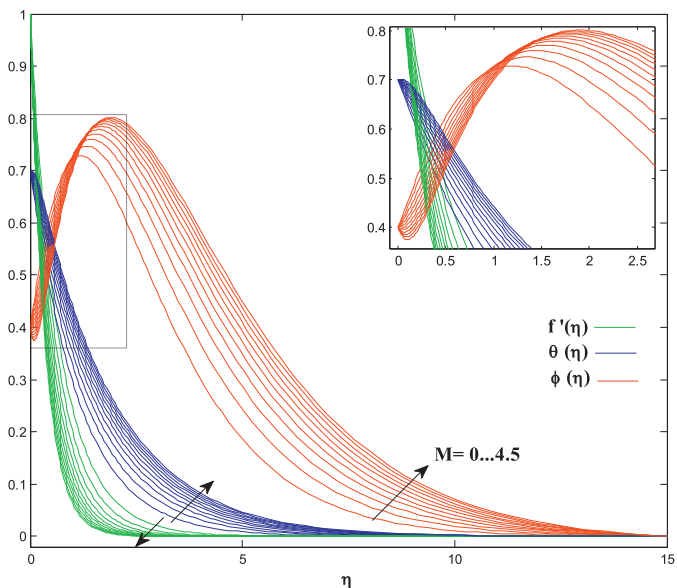


Fig. 2. Effects of  $M$  on velocity  $f(\eta)$ , temperature  $\theta(\eta)$  and concentration profile  $\varphi(\eta)$ .

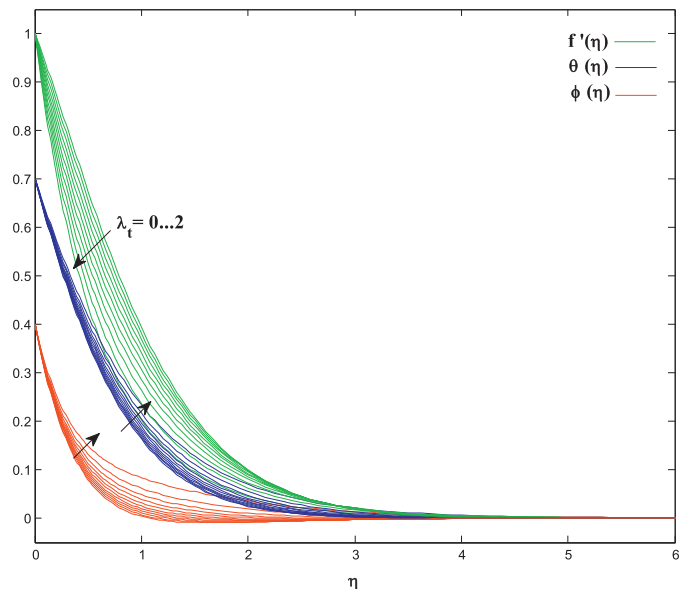


Fig. 4. Effects of  $\lambda_t$  on velocity  $f(\eta)$ , temperature  $\theta(\eta)$  and concentration profile  $\varphi(\eta)$ .

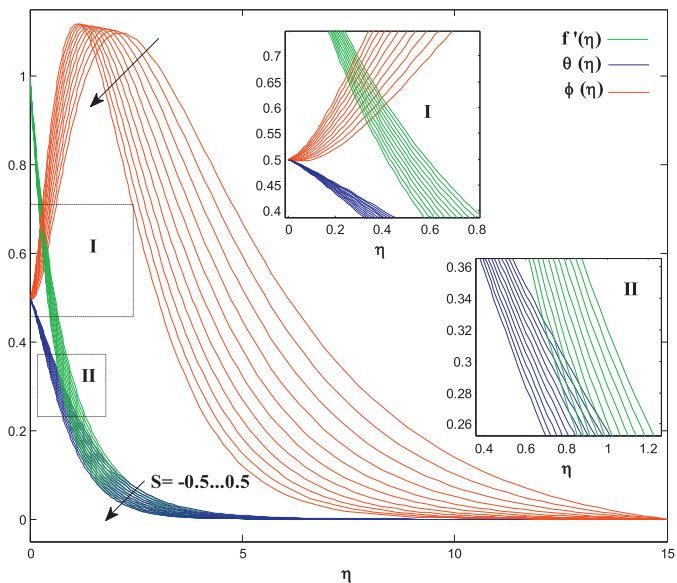


Fig. 3. Effects of  $S$  on velocity  $f(\eta)$ , temperature  $\theta(\eta)$  and concentration profile  $\varphi(\eta)$ .

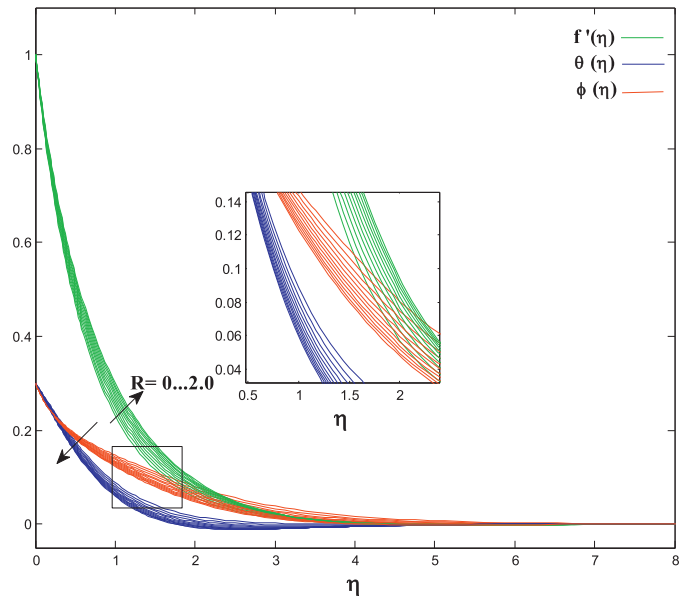


Fig. 5. Effects of  $R$  on velocity  $f(\eta)$ , temperature  $\theta(\eta)$  and concentration profile  $\varphi(\eta)$ .

profile have similar but minor variation with decreasing behaviour. Figs. 5 and 6, demonstrate the influence of  $\lambda_t$  and  $R$  on each velocity, temperature and concentration. Both  $\lambda_t$  and  $R$  have opposite influence on each of the velocity, temperature and concentration profile. Fig. 6 shows the variation in temperature and concentration profiles against the similarity variable  $\eta$  with the influence of thermal stratification parameter  $\varepsilon_1$ . Here, it is found that temperature profile considerably decreases as the thermal stratification parameter  $\varepsilon_1$  increases. This relation often occurs when heat is transfer from hot to the cold region and concentration is depicts the same behaviour. It can further observe from Fig. 6 that temperature distribution is scattered at the surface ( $\eta=0$ ) with respect to various values of stratification parameter. Thermal stratification parameter effect the temperature profile in such a way that decrease in surface temperature or increase in ambient temperature. Further temperature profile is reduced due to tempera-

ture difference is gradually decreasing between ambient fluid and surface of sheet. Therefore thermal boundary layer thickness decreases for higher values of thermal stratification  $\varepsilon_1$ . Fig. 7 depicts the influence of  $\varepsilon_2$  on  $\theta(\eta)$  and  $\varphi(\eta)$ . It is determined that  $\varphi(\eta)$  decreasing with increasing values of solutal stratified parameter  $\varepsilon_2$ . Increase in solutal stratification  $\varepsilon_2$  reduces the concentration difference between sheet and ambient fluid and hence concentration decreases. It is also concluded from Fig. 7, that temperature is slightly decreasing with increasing values of solutal stratification parameter  $\varepsilon_2$ .

The Brownian motion of the nanoparticles is significant factors to improve the proficiency of heat transfer when nanoparticles are incorporated within the base fluid. Due to this random motion, nanoparticles collide with each other and transfer the kinetic energy from one to another particle. Based upon this phenomenon heat is transfer due to random motion of nanoparticles.



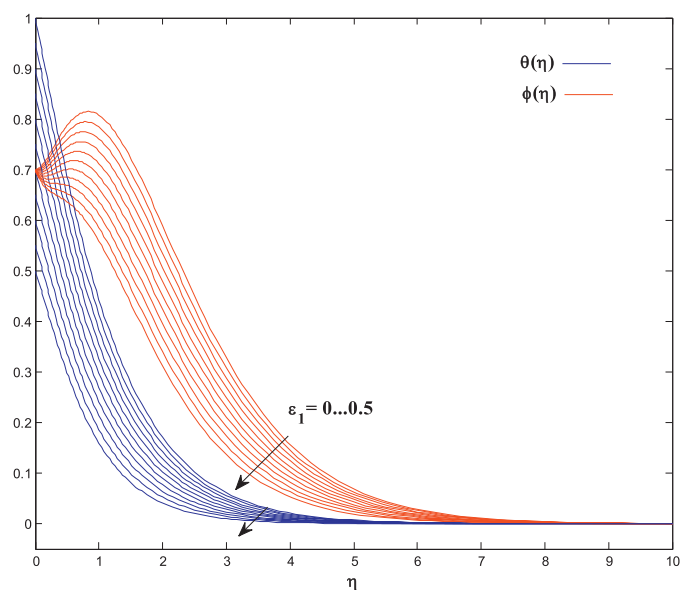


Fig. 6. Effects of  $\varepsilon_1$  on temperature  $\theta(\eta)$  and concentration profile  $\varphi(\eta)$ .

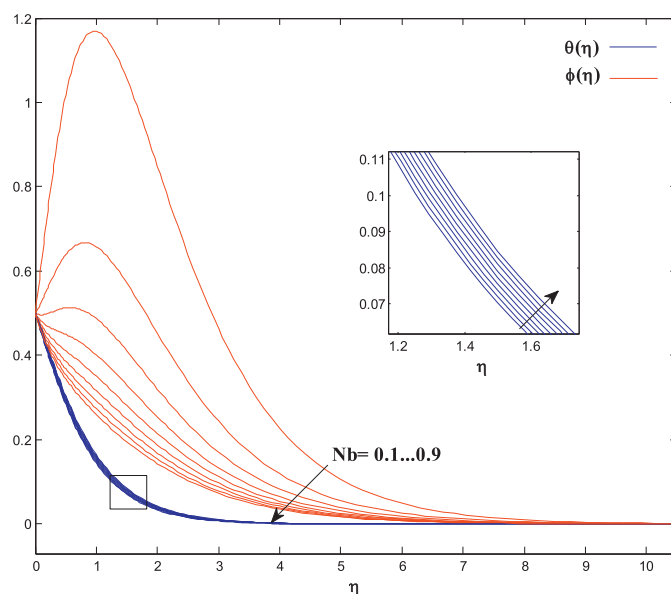


Fig. 8. Effects of  $Nb$  on temperature  $\theta(\eta)$  and concentration profile  $\varphi(\eta)$ .

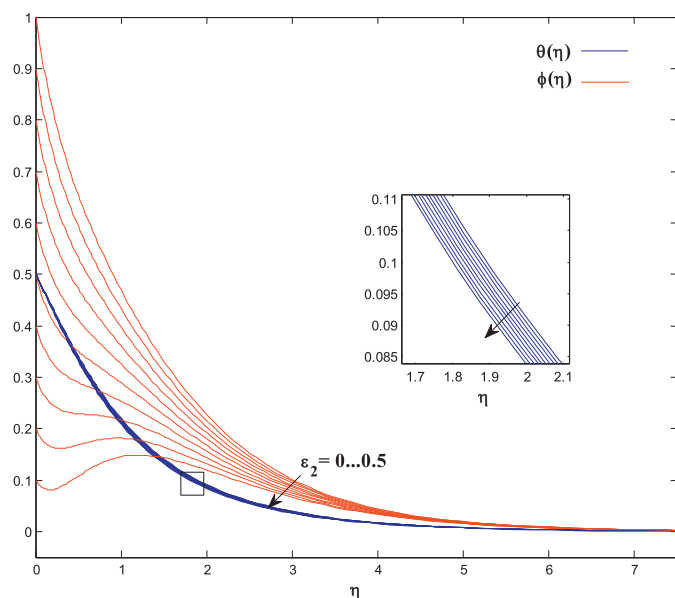


Fig. 7. Effects of  $\varepsilon_2$  on temperature  $\theta(\eta)$  and concentration profile  $\varphi(\eta)$ .

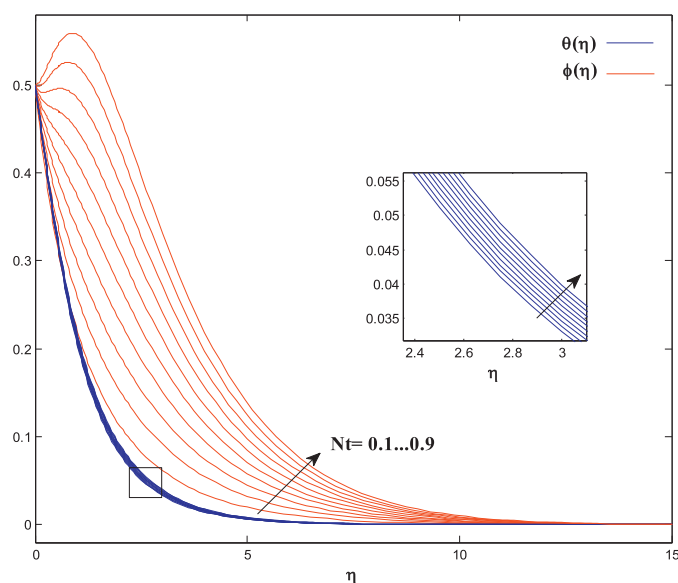


Fig. 9. Effects of  $Nt$  on temperature  $\theta(\eta)$  and concentration profile  $\varphi(\eta)$ .

Fig. 8 demonstrate the consequence of Brownian motion  $Nb$  on  $\theta(\eta)$  and  $\varphi(\eta)$ . It is found that increase of  $Nb$  provides the slight enhancement in heat transfer within the boundary layer region. While, effect of  $Nb$  illustrate opposite trend for concentration. It is important to note that both concentration and thermal boundary layer thickness decrease with increasing values of Brownian motion parameter  $Nb$ . Fig. 9 is plotted to discuss the effect of thermophoretic parameter  $Nt$  on temperature  $\theta(\eta)$  and concentration profile  $\varphi(\eta)$  for fixed values of other parameters. It is found that increase in thermophoretic parameter  $Nt$  leads to enhance both the fluid temperature and concentration. Temperature gradient generates the thermophoresis force which creates a fast flow away from the sheet.

To analyse the friction of fluid at the surface we have plotted the skin friction coefficient for emerging parameters  $M$  and  $S$  (see Fig. 10). One can observe that absolute value of skin friction at the surface of the sheet increases as we increase Hartmann number  $M$  for both suction and injection case. This behaviour predicts due

to drag force known as Laurent force which produces resistance in the motion of the fluid particles and this effect is more influenced when fluid contained nanoparticles. It is further acquired that this increasing behaviour also maintained for increasing values of suction/injection parameter  $S$ . In order to obtain the heat transfer and concentration at the surface with respect to suction/injection parameter  $S$  and Hartmann number  $M$ , we have plotted the local Nusselt and Sherwood number in Fig. 11. In view of both suction and injection case both Nusselt number and Sherwood number has same increasing behaviour. Since Hartmann number is ratio of electromagnetic force to viscous force there for when we increase the values of Hartmann number then electromagnetic force have dominant effect to reduce the heat transfer rate at the surface. Due to electromagnetic force nanoparticles accumulate at the surface of the sheet and effect the concentration at the surface. As a result Sherwood number increases with respect to the increasing values of Hartmann number. Effects of thermally stratified parameter  $\varepsilon_1$  and solutal stratified parameter  $\varepsilon_2$  on both Nusselt and Sherwood number are plotted in Figs. 12 and 13. One can

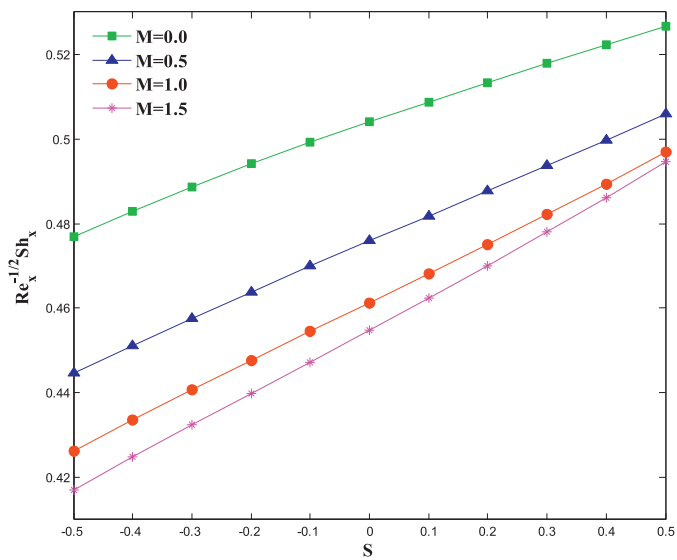


Fig. 10. Variation of skin friction and Nusselt with respect to the various values of  $M$  and  $S$  when  $Pr=1$ ,  $Le=0.7$ ,  $R=Ec=\lambda=0.5$ ,  $\varepsilon_1=0.3$ ,  $\varepsilon_2=0.5$ ,  $Nb=0.7$ , and  $Nt=0.3$ .

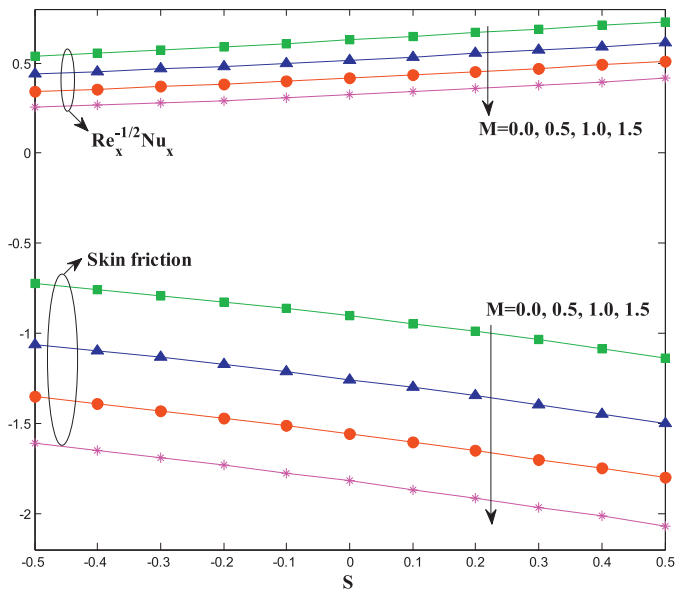


Fig. 11. Variation of Sherwood number for various values of  $M$  and  $S$  when  $Pr=1$ ,  $Le=0.7$ ,  $R=Ec=0.5$ ,  $\varepsilon_1=0.3$ ,  $\varepsilon_2=0.5$ ,  $Nb=0.7$ , and  $Nt=0.3$ .

see that both thermal and solutal stratified parameter have opposite effects on Nusselt and Sherwood number. Since thermally stratified refer to change in temperature at different depth of the boundary layer. If bottom of the wall is heated then due to change in density cold fluid will accumulate at the bottom of the wall and fluid will loss the kinetic energy and consequently Nusselt number gives decreasing behaviour with respect to thermally stratified parameter. However effects of thermally stratified parameter on Sherwood number are quite opposite. In Fig. 14, results of Nusselt and Sherwood number are obtained against  $Nb$  and  $Nt$ . As we can see that Nusselt and Sherwood number are decreasing functions of thermophoresis parameter due to loss of concentration at the surface. Since Brownian motion is the random motion of nanoparticles so increase in the Brownian motion give the loss of kinetic energy and hence it will decrease the heat transfer at the surface and raise the Sherwood number.

In Table 2, we have presented the variations of  $-\theta'(0)$  and  $-\phi'(0)$  for different values of important physical parameter. From

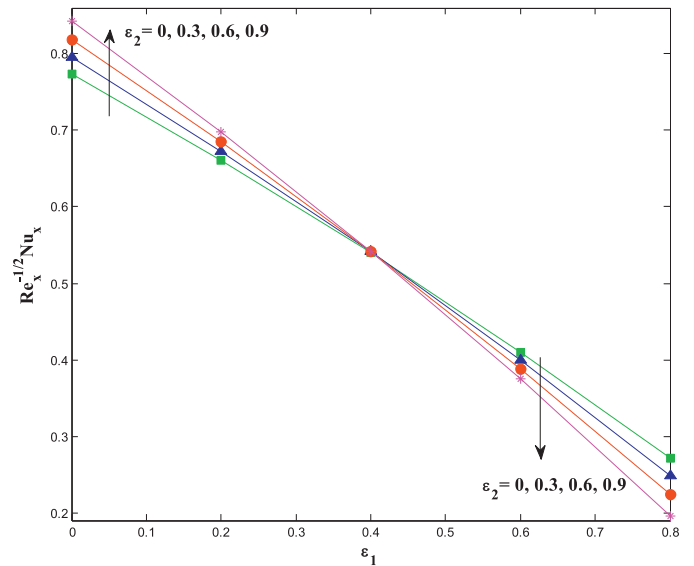


Fig. 12. Variation of Nusselt number for various values of  $\varepsilon_1$  and  $\varepsilon_2$ .

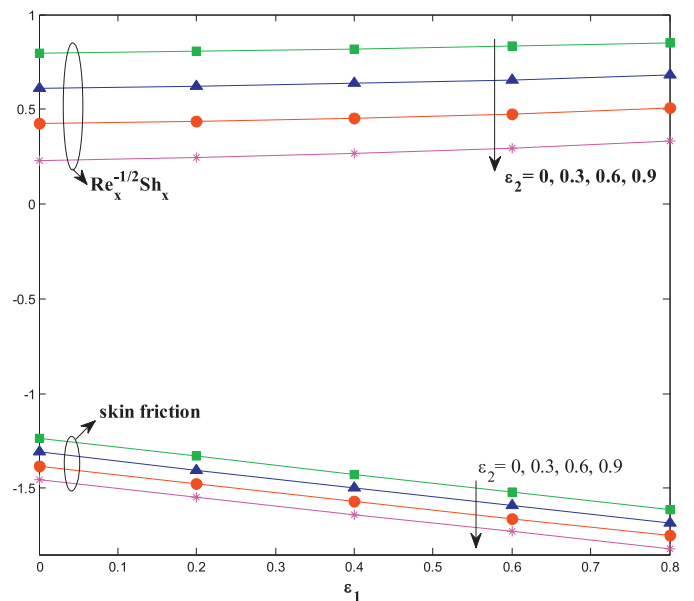


Fig. 13. Variation of skin friction and Sherwood number for various values of  $\varepsilon_1$  and  $\varepsilon_2$ .

Table 2

Numerical values of Nusselt and Sherwood number for various values of  $\varepsilon_1$ ,  $\varepsilon_2$ ,  $Nt$ ,  $Nb$  and  $Ec$  when  $Pr=0.7$ ,  $S=M=\lambda_i=R=0.5$  and  $Le=1$  are fixed.

$\varepsilon_1$	$\varepsilon_2$	$Nt$	$Nb$	$Ec$	$-\theta'(0)$	$-\phi'(0)$
0.3	0.3	0.3	0.3	0.1	0.77200	-0.11024
0.5	0.3	0.3	0.3	0.1	0.65739	-0.05778
0.7	0.3	0.3	0.3	0.1	0.53318	0.00582
0.7	0.5	0.3	0.3	0.1	0.51782	-0.06035
0.7	0.7	0.3	0.3	0.1	0.50126	-0.12586
0.7	0.7	0.5	0.3	0.1	0.51502	-0.42108
0.7	0.7	0.7	0.3	0.1	0.52658	-0.72358
0.7	0.7	0.7	0.5	0.1	0.49844	-0.28654
0.7	0.7	0.7	0.7	0.1	0.48205	-0.10701
0.7	0.7	0.7	0.7	0.2	0.43670	-0.06241
0.7	0.7	0.7	0.7	0.3	0.39165	-0.01813

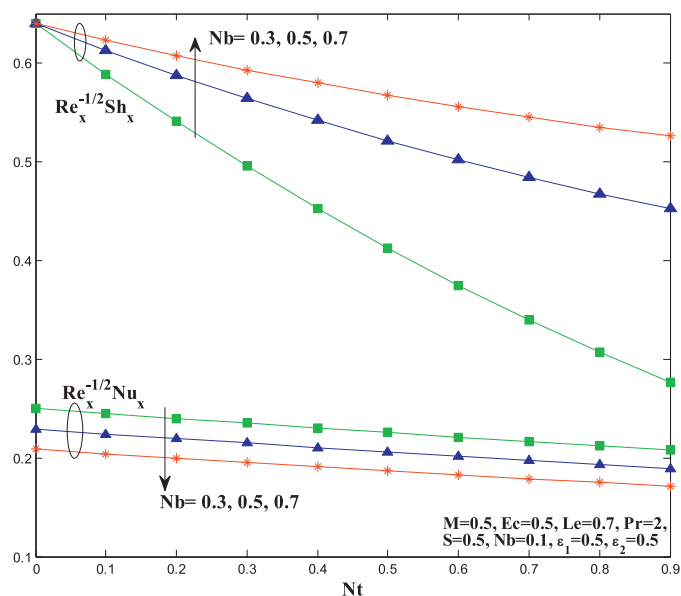


Fig. 14. Variation of Nusselt and Sherwood number for various values of  $Nb$  and  $Nt$ .

the table we can conclude that increasing values of each physical parameter, Nusselt number obtains the decreasing behaviour. It can further conclude that Sherwood number is increasing function of  $\varepsilon_1$ ,  $Nb$  and  $Ec$  and decreasing function of  $\varepsilon_2$  and  $Nt$ .

#### 4. Conclusions

In this paper numerical study of thermally stratified MHD flow of nanofluid over an exponentially stretching sheet with joule heating and viscous dissipation has been presented. Transformed nonlinear ODEs are solved by implicit finite difference scheme. The main findings of this study are presented below.

- Temperature and concentration profiles are reduced with an increase in thermally stratified parameter.
- Solutal stratified parameter reduces the concentration profile.
- Temperature profile enhanced with an increase in Eckert number.
- Concentration profile reduced with the various values of Prandtl number.
- Thermophoresis exhibits the increasing behaviour for both temperature and nanoparticle concentration profile.

#### Acknowledgement

1. Authors would like to acknowledge and express their gratitude to the United Arab Emirates University, Al Ain, UAE for providing the financial support with Grant No. 31S212-UPAR (9)2015.

2. The first author is very thankful to University Grants Commission, India, for providing the opportunity to do this research work under UGC - Faculty Development Programme (FDP), India.

#### References

- [1] Sakiadis BC. Boundary-layer behavior on continuous: I. boundary layer equations for two-dimensional and axisymmetric flow. *J Am Inst Chem Eng* 1961;7:26–8.
- [2] Crane LJ. Flow past a stretching plate. *Zeit Angew Math Phys* 1970;21:645–7.
- [3] Gupta PS, Gupta AS. Heat and mass transfer on a stretching sheet with suction or blowing. *Can J Chem Eng* 1977;55:744–6.
- [4] Gupta BK, Roy P, Gupta AS. Temperature field in the flow over a stretching sheet with uniform heat flux. *Int Commun Heat Mass Transf* 1985;12:89–94.
- [5] Chen CK, Char MI. Heat transfer of a continuous stretching surface with suction or blowing. *J Math Anal Appl* 1988;135:568–80.

- [6] Magyari E, Keller B. Heat and mass transfer in the boundary layers on an exponentially stretching continuous surface. *J Phys D Appl Phys* 1999;32:577–85.
- [7] Elbashareshy EMA. Heat transfer over an exponentially stretching continuous surface with suction. *Arch Mech* 2001;53:643–51.
- [8] Partha MK, Murthy PVS, Rajasekhar GP. Effect of viscous dissipation on the mixed convection heat transfer from an exponentially stretching surface. *Heat Mass Transf* 2005;41:360–6.
- [9] Khan SK, Sanjayanand E. Viscoelastic boundary layer flow and heat transfer over an exponential stretching sheet. *Int J Heat Mass Trans* 2005;48:1534–42.
- [10] Sanjayanand E, Khan SK. On the heat and mass transfer in a viscoelastic boundary layer flow over an exponentially stretching sheet. *Int J Therm Sci* 2006;45:819–28.
- [11] Bidin B, Nazar R. Numerical solution of the boundary layer flow over an exponentially stretching sheet with thermal radiation. *Eur J Sci Res* 2009;33:710–17.
- [12] Al-Odat MQ, Damesh RA, Al-Azab TA. Thermal boundary layer on an exponentially stretching continuous surface in the presence of magnetic field effect. *Int J Appl Mech Eng* 2006;11:289–99.
- [13] Sajid M, Hayat T. Influence of thermal radiation on the boundary layer flow due to an exponentially stretching sheet. *Int Commun Heat Mass Transf* 2008;35:347–56.
- [14] Ishak A. MHD boundary layer flow due to an exponentially stretching sheet with radiation effect. *Sains Malays* 2011;40:391–5.
- [15] Bhattacharyya K. Slip effects on boundary layer flow and mass transfer with chemical reaction over a permeable flat plate in a porous medium. *Front Heat Mass Transf (FHMT)* 2012;3:043006.
- [16] Choi SUS. Enhancing thermal conductivity of fluids with nanoparticles. In: *Proceedings of the 1995 international mechanical engineering congress and exhibition*, 66; 1995. p. 99–105. ASME FED 231/MD.
- [17] Keblinski P, Eastman JA, Cahill DG. Nanofluids for thermal transport. *Mater Today* 2005;8(6):36–44.
- [18] Buongiorno J. Convective transport in nanofluids. *Trans ASME* 2006;128:240–50.
- [19] Daughthongsuk W, Wongwises S. A critical review of convective heat transfer nanofluids. *Renew Sust Eng Rev* 2007;11:797–817.
- [20] Wang XQ, Mujumdar AS. A review on nanofluids – Part I: theoretical and numerical investigations. *Braz J Chem Eng* 2008;25:613–30.
- [21] Wang XQ, Mujumdar AS. A review on nanofluids – Part II: experiments and applications. *Braz J Chem Eng* 2008;25:631–48.
- [22] Kakac S, Pramuanjaroenkij A. Review of convective heat transfer enhancement with nanofluids. *Int J Heat Mass Transf* 2009;52:3187–96.
- [23] Kuznetsov AV, Nield DA. Natural convective boundary layer flow of a nanofluid past a vertical plate. *Int J Therm Sci* 2010;49:243–7.
- [24] Khan WA, Pop I. Boundary layer flow of a nanofluid past a stretching sheet. *Int J Heat Mass Transf* 2010;53:2477–83.
- [25] Makinde OD, Aziz A. Boundary layer flow of a nanofluid past a stretching sheet with a convective boundary condition. *Int J of Therm Sci* 2011;50(7):1326–32.
- [26] Ibrahim W, Shanker B. Boundary layer flow and heat transfer of nanofluid over a vertical plate with convective surface boundary condition. *J Fluid Eng Trans ASME* 2012;134:081201–3.
- [27] Rana P, Bhargava R. Flow and heat transfer of a nanofluid over a nonlinearly stretching sheet: a numerical study. *Commun Nonlinear Sci Numer Simul* 2012;17(1):212–26.
- [28] Hady FM, Ibrahim FS, Abdel-Gaied SM, Eid MR. Radiation effect on viscous flow of a nanofluid and heat transfer over a nonlinearly stretching sheet. *Nanoscale Res Lett* 2012;7:229.
- [29] Makinde OD, Khan WA, Khan ZH. Buoyancy effects on MHD stagnation point flow and heat transfer of a nanofluid past a convectively heated stretching/shrinking sheet. *Int J Heat Mass Transf* 2013;62:526–33.
- [30] Bachok N, Ishak A, Pop I. Unsteady boundary layer flow and heat transfer of a nanofluid over a permeable stretching/shrinking sheet. *Int J Heat Mass Transf* 2012;55:2102–9.
- [31] Nadeem S, Lee C. Boundary layer flow of nanofluid over an exponentially stretching surface. *Nanoscale Res Lett* 2012;7:1–15.
- [32] Mustafa M, Hayat T, Obaidat S. Boundary layer flow of a nanofluid over an exponentially stretching sheet with convective boundary conditions. *Int J Numer Methods Heat Fluid Flow* 2013;23(6):945–59.
- [33] Nadeem S, Haq RUI, Khan ZH. Heat transfer analysis of water-based nanofluid over an exponentially stretching sheet. *Alex Eng J* 2014;53(1):219–24.
- [34] Alim MA, Alam MD, Mamun A. Joule heating effect on the coupling of conduction with magneto hydrodynamic free convection flow from a vertical flat plate. *Nonlinear Anal Model Control* 2007;12(3):307–16.
- [35] Duwairi HM. Viscous and joule heating effects on forced convection flow from radiate isothermal porous surfaces. *Int J Numer Methods Heat Fluid Flow* 2005;15(5):429–40.
- [36] Yang KT, Novotny JL, Cheng YS. Laminar free convection from a non-isothermal plate immersed in a temperature stratified medium. *Int J Heat Mass Transf* 1972;15:097–1109.
- [37] Jaluria Y, Gebhart B. Stability and transition of buoyancy induced flows in a stratified medium. *J Fluid Mech* 1974;66:593–612.
- [38] Chen CC, Eichhorn R. Natural convection from simple bodies immersed in thermally stratified fluids. *ASME J Heat Transf* 1976;98:446–51.

- [39] Kulkarni AK, Jacobs HR, Hwang JJ. Similarity solution for natural convection flow over an isothermal wall immersed in thermally stratified medium. *Int J Heat Mass Transf* 1987;30:681–8.
- [40] Ishak A, Nazar R, Pop I. Mixed convection boundary layer flow adjacent to a vertical surface embedded in a stable stratified medium. *Int J Heat Mass Transf* 2008;51:3693–5.
- [41] Rosmila AB, Kandasamy R, Muhaimin I. Lie symmetry group transformation for MHD natural convection flow of nanofluid over linearly porous stretching sheet in presence of thermal stratification. *Appl Math Mech Engl Ed* 2012;33:593–604.
- [42] Ibrahim W, Makinde OD. The effect of double stratification on boundary layer flow and heat transfer of nanofluid over a vertical plate. *Comput Fluids* 2013;86:433–41.
- [43] Shehzad SA, Qasim M, Alsaedi A, Hayat T, Alhothuali MS. Combined thermal stratified and thermal radiation effects in mixed convection flow of a thixotropic fluid. *Eur Phys J Plus* 2013;128:7.
- [44] Mukhopadhyay S. MHD boundary layer flow and heat transfer over an exponentially stretching sheet embedded in a thermally stratified medium. *Alex Eng J* 2013;52(3):259–65.
- [45] Cebeci T, Bradshaw P. *Physical and computational aspects of convective heat transfer*. Springer-Verlin; 1984.